11th World Congress on Computational Mechanics (WCCM XI)
5th European Conference on Computational Mechanics (ECCM V)
6th European Conference on Computational Fluid Dynamics (ECFD VI)
E. Oñate, J. Oliver and A. Huerta (Eds)

FAILURE MECHANISMS OF LIGHT ALLOYS WITH A BIMODAL GRAIN SIZE DISTRIBUTION

NATALYA V. SKRIPNYAK[*], EVGENIYA G. SKRIPNYAK[*],

VLADIMIR A. SKRIPNYAK[*,†], VLADIMIR V. SKRIPNYAK[*], IRINA K. VAGANOVA[*]

[*] Tomsk State University, Lenin av. 36, 634050, Tomsk, Russia,
skrp@ftf.tsu.ru and http://www.tsu.ru

[†] Institute of Strength Physics and Materials Sciences SB RAS, Academichisky av. 2/4, 634021
Tomsk, Russia skrp@yandex.ru and http://www.ispms.ru

Key Words: *Fracture, Light Alloy, Grain Size, Probability, 3-D model, Elastic-plastic Body, Multiscale Simulation.*

Abstract. Physical mechanisms of dynamic fracture of ultrafine-grained (UFG) light alloys were investigated by numerical simulation method. The multiscale level approach has been used for computer simulation of magnesium and aluminium alloys response to tension and compression at high strain rates. The model structured representative volumes (RVE) takes into account the influence of unimodal and bimodal grain size distributions and concentration of precipitates on mechanical properties of alloys.
Fracture of fine-grained alloys under dynamic loading has probabilistic character and depends on parameters of structure heterogeneity. Damage nucleation is associated with strain localization at mesoscale level. Results of computer simulation demonstrate that the high strain localization in UFG alloys under dynamic loadings depends on the ratio between volume concentrations of small and coarse grains. Fine precipitates in alloys not only affect the hardening but also lead to change the influence of the grains size distribution on volume concentration of shear bands.

1 INTRODUCTION

The grains structure influence on mechanical properties of light alloys after severe plastic deformation have been investigating over last 10 years [1-5]. Results of researches testify that reduction in the average size of grain of aluminum, magnesium, and titanium alloys causes enhanced strength and ductility under quasi-static loading conditions [6,7]. It was revealed that grains of nanostructured (NS) and ultrafine-grained (UFG) alloys have size distributions. Unimodal distributions of grain sizes in bulk UFG alloys can be approximated by the lognormal or the Weibull laws. It was noticed that grain size distributions influence on plastic flow stress and strength at compression and tension, elongation to fracture [6,7]. Fan [8], Ahn [9], Lee [10], Han [11,12] showed that the bimodal grain distribution can be formed in light alloys by means of severe plastic deformation and follow-up heat treatment.

It was revealed that UFG aluminum and magnesium alloys with a bimodal grain size distribution exhibit a number of anomalies in mechanical behavior. In these alloys, there is a negative strain rate sensitivity of plastic flow stress and increase in ductility with strain rate growth in a range of 10^{-4} to 1 s^{-1} [8-12].

Increased cracks growth resistance in Al-Mg alloys with a bimodal grain size distribution is a result of deflection of microcracks on borders between UFG and coarse grained (CG) zones [10]. As a result of it, resistance to cracks growth at mesoscale level increases with increasing macroscopical plastic deformation.

Features of mechanical behavior of UFG light alloys with bimodal grain sizes distribution is defined by shear bands formation, nucleation and growth of damages, coalescence damages under formation of mesoscale and macroscale cracks.

Therefore, processes of shear banding in light UFG alloys with bimodal and unimodal grain size distributions depend on strain rates. The mechanisms of dynamic fracture in light alloys with bimodal grain size distributions are poorly investigated. We present computational model and results of numerical simulation of damaging and fracture of aluminium and magnesium alloys under dynamic loading.

2 PROBLEM STATEMENT, CONSTITUTIVE EQUATIONS, AND FRACTURE MODEL.

The multilevel computer simulation method was used for numerical research on damage and formation of cracks within structured representative volume element (RVE) of the alloy [13,14].

Several types of grain structure that take place in light alloys after severe plastic deformation were simulated. Grain size distributions of aluminium and magnesium alloys after various numbers of passes of equal channel angular pressing (ECAP) is reported in [1-12, 15-17]. The analysis of grain structure distributions has shown that there are several types of grains structure. The model structured RVE of alloys was created using the experimental data on grains structures. Fig.1 shows sections of RVE with a quasi-regular grains structure (a), and bimodal grain sizes distributions with specific volume of coarse grains of 38 % (b), and 75 % (c), respectively.

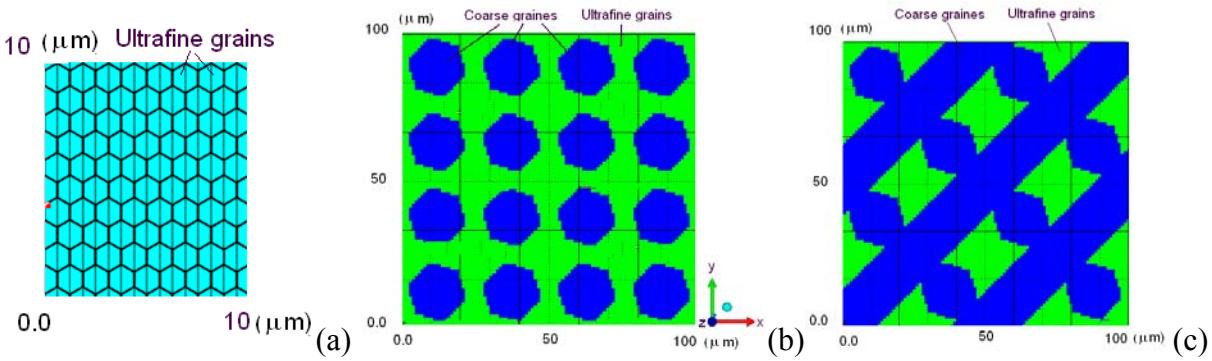

Fig. 1. Model of grains distribution in RVE.

Models RVE have the volume fracture of coarse grains: 0, 5, 10, 15, 30, 50, 75, and 100 %. When volume fracture of coarse grains exceeds the percolation limit (~0.2 − 0.25) the cell grain structures were takes into consideration. Mechanical behavior of alloy is described by

means of averaging the mechanical response of structured RVE at mesoscale level under loading of high strain rates. 3D models of representative volume element (RVE) of alloys with a bimodal grain size distribution have dimension 100x100x5 $(\mu m)^3$.

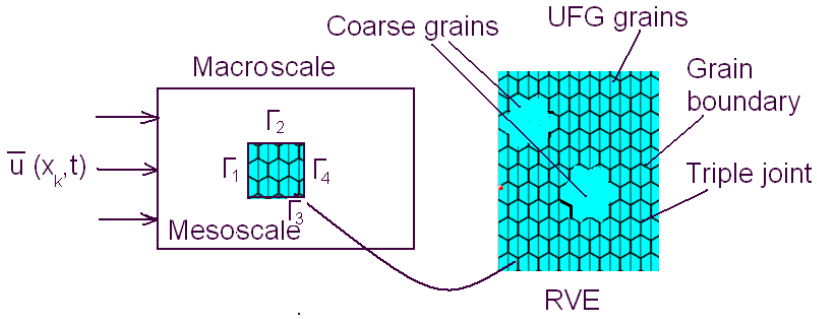

Fig. 2. Boundary conditions for RVE under dynamic loadings.

Smooth particles hydrodynamic (SPH) method was used for the simulation [18]. Therefore, using the kinematic boundary conditions were preferably. The kinematic boundary conditions correspond to combination of compression, shear, and tension. The scheme of boundary conditions is shown in Fig. 2.

$$u_k(x_k,t)=u_k(x_k,t) \quad x_k \in \Gamma_4, x_k \in \Gamma_2, x_k \in \Gamma_3 \ . \tag{1}$$

where u_k are components of particle velocity vector, t is time, x_k are Cartesian coordinates.

Mechanical behavior at mesoscale level is described within approach of damaged elastic-plastic medium. Kinematics of medium was described by the local strain rate tensor:

$$\dot{\varepsilon}_{ij}=\frac{1}{2}(\nabla_i u_j+\nabla_j u_i) \ , \tag{2}$$

where $\dot{\varepsilon}_{ij}$ are components of the strain rate tensor, u_i are components of particles velocity vector, ∇_i is Hamilton operator.

Components of strain rate tensor are expressed by sum of elastic and inelastic terms:

$$\dot{\varepsilon}_{ij}=\dot{\varepsilon}^{e}_{ij}+\dot{\varepsilon}^{n}_{ij} \ , \tag{3}$$

where $\dot{\varepsilon}^{e}_{ij}$ are components of the elastic strain rate tensor, $\dot{\varepsilon}^{n}_{ij}$ are components of the inelastic strain rate tensor.

The bulk inelastic strain rate is described by relation:

$$\dot{\varepsilon}^{n}_{kk}=\frac{1}{3}\frac{\dot{D}}{(1-D)} \ , \tag{4}$$

where D is the damage parameter, the substantial time derivative is denoted via dot notation.

The bulk inelastic strain rate $\dot{\varepsilon}^{n}_{kk}$ is equal to zero only when material is undamaged.

We consider the possibility of damage accumulation during inelastic deformation of UFG metals as a result of limited ductility. The local damage parameter D is introduced in the form:

$$D = \int_0^{t_f} \frac{\dot{\varepsilon}_{eq}^n}{\varepsilon_f^n} dt \tag{5}$$

where $\dot{\varepsilon}_{eq}^n = (\frac{2}{3}\dot{\varepsilon}_{ij}^n \dot{\varepsilon}_{ij}^n)^{1/2}$, ε_f^n is the threshold of inelastic strain, t_f.is the time before local fracture.

The local failure criterion for the condensed phase is :

$$D = 1. \tag{6}$$

Dynamics of structured RVE is described in Lagrange coordinate system by mass conservation, momentum conservation and energy conservation equations:

$$\frac{\partial \sigma_{ij}}{\partial x_j} = \rho \frac{du_i}{dt}, \ \frac{d\rho}{dt} = \rho \frac{\partial u_i}{\partial x_i}, \ \rho \frac{dE}{dt} = \sigma_{ij} \dot{\varepsilon}_{ij}, \tag{7}$$

where σ_{ij} are components of stress tensor, ρ is the mass density, u_i are components of particles velocity vector, ε_{ij} is components of strain rate tensor, E is the specific internal energy per unit mass.

We use the ductile fracture criteria for UFG light alloys at the room and elevated temperatures owing to relatively low melting temperature. (The melting temperature of aluminum and magnesium alloys is equal to~ 900 K).

It was assumed that total plastic work per unit volume for crystalline phase of light alloys is nearly constant [19]:

$$W^p = \int_0^{t_f} \sigma_{ij} \dot{\varepsilon}_{ij}^n \, dt = const \tag{8}$$

Two models of fracture prediction based on the criterion of Eq. (6) may be used. The first model uses Eq. (5) and phenomenological relation for the threshold inelastic strain ε_f^n :

$$\varepsilon_f^n = D_1 (P^* + T^*)^{D_2}, \tag{9}$$

where $T^* = \sigma_{sp}/P_{HEL}$, $P^* = p/P_{HEL}$, P_{HEL} is the pressure corresponding to the Hugoniot Elastic Limit, D_1, D_2 are material constants.

The second model uses Eqs. (4), (5), (8) and define the damage parameter by relation:

$$D = \frac{1}{C_1} \int_0^{\varepsilon_{f0}^n + k d_g^{-1/2}} exp(-\frac{p}{\sigma_{eq}} C_2) \, d\varepsilon_{eq}^n, \tag{10}$$

where d_g is the grain size of mesoscale region with the unimodal distribution of grain sizes, p is the pressure, ε_{f0}^n, k, C_1, C_2 are parameters of materials region with the unimodal grain size distribution, $e_{ij}^p = [(2/3) e_{ij}^n e_{ij}^n]^{1/2}$, $\varepsilon_{ij}^n = (1/3)\varepsilon_{kk}^n \delta_{ij} + e_{ij}^n$, $\sigma_{eq} = [3/2 S_{ij} S_{ij}]^{1/2}$, $\sigma_{ij} = -p\delta_{ij} + S_{ij}$, δ_{ij} is the Kronecker delta,

The constitutive equation of material particles is written in the form:

$$\sigma_{ij} = \sigma_{ij}{}^{(m)} \varphi(D),\ \sigma^{(m)}{}_{ij} = -p^{(m)} \delta_{ij} + S_{ij}{}^{(m)}, \tag{11}$$

where σ_{ij}, p, and S_{ij} are the stress tensor, pressure, and deviator of the stress tensor, respectively, the superscript m indicates the condensed phase of the damaged material, $\varphi(D) \approx 1\text{-}D$ is the function of damage, and D is the damage parameter.

The pressure is calculated by polynomial equation of state [20].

The stress tensor deviator is calculated by the equation:

$$d S^{(m)}{}_{ij} / d t = 2\mu(\dot{e}_{ij} - \dot{e}_{ij}{}^{p}), \tag{8}$$

where *d /dt* is the Jaumann derivative, μ is the shear modulus, $\dot{e}_{ij}$ is the deviator of the strain rate tensor, and $\dot{e}^{n}_{ij}$ is the deviator of the inelastic strain rate tensor.

The deviator of the inelastic strain rate tensor is written as:

$$\dot{e}^{p}_{ij} = (3/2)[S_{ij}\, \dot{e}^{p}_{eq} / \sigma_{eq}], \tag{9}$$

where $\sigma_{eq} = [(3/2) S_{ij} S_{ij}]^{1/2}$.

The scalar function $\dot{e}^{p(m)}_{eq}$ is defined by the sum of components based on physical mechanisms of inelastic deformation by relations:

$$\dot{e}^{p}_{eq} = [\dot{e}^{p}_{eq}]_{disl} + [\dot{e}^{p}_{eq}]_{disl\ nucl} + [\dot{e}^{p}_{eq}]_{tw}, \tag{10}$$

where $[\dot{e}^{p}_{eq}]_{disl}$, $[\dot{e}^{p}_{eq}]_{disl\ nucl}$, $[\dot{e}^{p}_{eq}]_{tw}$ are inelastic strain rates caused by dislocation movement, dislocation nucleation, and twinning, respectively.

Peculiarity of deformation laws of FCC and HCP groups of light metals should be described by different kinetic equations (11):

$$[\dot{e}^{p}_{eq}]_{disl\ mov} = g b v \rho_m \exp(-\Delta G_1 / RT),\ v = v_s\left(\frac{\sigma_{eff}{}^{2}}{1+\sigma_{eff}{}^{2}}\right), \Delta G_1 = \Delta G_0 [1 - (\sigma_{eq} / \sigma^{*}_{eq})^{n_1}]^{q},$$

$$\rho_m = [\rho^{*} + (\rho_0 + \rho_{nucl} - \rho^{*}) \exp(-A \varepsilon^{p}_{eq})][f^{*} + (f^{*} - f_0) \exp(-B \varepsilon^{p}_{eq} \frac{1-\rho}{\rho^{*}})],$$

$$\sigma_{eff} = \sigma_{eq} - \Delta\sigma_{bs}, \Delta\sigma_{bs} = k_1 d_g{}^{-1/2} + k_2 (\varepsilon^{P}_{eq})^{1/2} + \Delta\sigma_{bs\,pr},$$

$$[\dot{e}^{p}_{eq}]_{disl\ nucl} = g\, b\, \dot{\rho}_{nucl}\, l_0 \exp(-\Delta G_2 / kT), \tag{11}$$

$$\dot{\rho}_{nucl} = (p + (2/3)\sigma_{eq})^{4} H[p + (2/3)\sigma_{eq} - \sigma_{HEL}],\ \rho_{nucl} = \int_0^t \dot{\rho}_{nucl} dt,$$

$$[\dot{e}^{p}_{eq}]_{tw} = A_{tw} \exp(-\Delta G_3 / RT)[1 - \sigma_{eff} / \sigma^{**}(d_g, T, P)]^{m_1},$$

$$\sigma^{*}_{eq} = \sigma^{*}_{eq0} + k d_g{}^{-1/2},\ \sigma^{**} = \sigma^{*}_{0} + k_1 d_g{}^{-1/2} + k_2 (\varepsilon^{P}_{eq})^{1/2} + k_3 p^{1/2},$$

where *T* is a temperature, *b* is the modulus of Burger's vector, $g \approx 0{,}5$ is the orientation coefficient, *v* is the average dislocation velocity, v_s is the shear sound velocity, G_0 and G_2 are specific activation energy of dislocation's movement and nucleation, respectively, $l_0 \sim 100$ nm is the average size of nucleated dislocation loops, *R* is the gas constant, *k* is Boltzmann's

constant, G_3 is specific activation energy of twinning, d_g is the grain size, ρ_m is the density of movable dislocations, f is a part of movable dislocations, $\dot{\rho}$ is the rate of dislocation's nucleation, A_{tw}, n_1, m_1, q, A, B are material constants, H[.] is the Heaviside function, $\Delta\sigma_{bs\,pr}$ is the internal stress from Orovan dislocation lops around precipitates.

Kinetic equations can be used in phenomenological relations forms [13-14, 21]:

Constants n, q, ΔG_0, ΔG_2 are different for aluminum alloys (FCC metal group) and magnesium alloys (HCP metals group) [22]. For aluminum alloys $[\dot{e}^p_{eq}]_{tw}$ is negligible.

The precipitate hardening of light alloys grains is described by the equation [23]:

$$\Delta\sigma_{bs\,pr} = 0.4\mu bM\, ln(2r/b)/(\pi\lambda\sqrt{1-\nu}), \qquad \lambda = (\sqrt{3\pi/4f} - 1.64)r, \tag{12}$$

where M is the material constant, r is the radius of particles, f is the concentration of particles, and ν is Poisson's ratio.

Average, current configuration, local lattice energy density values in grain boundary and triple point regions are compared.

The researches of failure mechanisms of light alloys with a bimodal grain size distribution was carried out for aluminum-magnesium alloy AMg6 (this is analog to Al 6061), and magnesium alloy Ma2-1 (this is analog to AZ31 magnesium alloy). In Ref. [24-27], numerical values of model parameters of UFG alloys are discussed. Used numerical method is discussed in [24-25].

3 RESULT AND DISCUSSION

Figure 3 shows damage and total plastic work per unit volume under tension at strain rate of 10^6 s^{-1} in RVE of UFG aluminum alloy with a bimodal distribution of grain size for given specific volume of coarse grains (grain size is equal to 20 μm) of ~5.5 %.

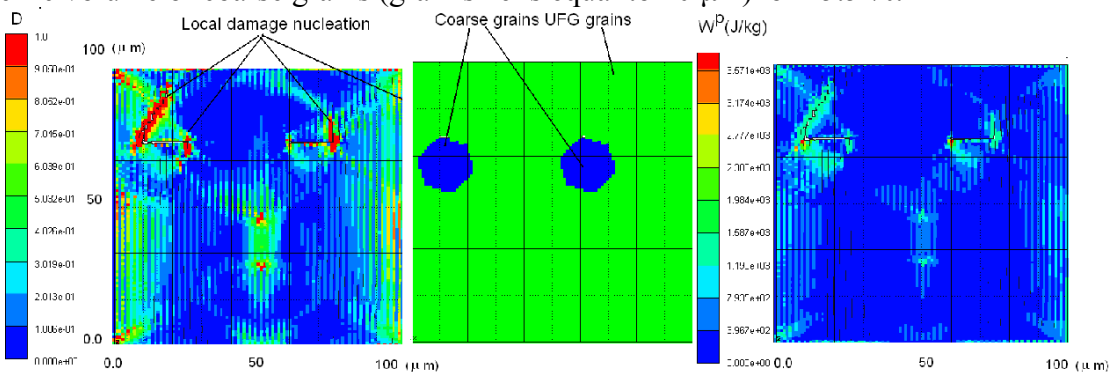

(a) (b) (c)

Fig. 3. Damage (a), RVE structure (b), and total plastic work per unit volume (c) in AMg6 aluminum alloy with coarse grain size of~20 μ and ultrafine grain size of~1 μm.

The duration of tension corresponds to 0.04 μs. It was assumed that average grain size of UFG volume is equal to ~1 μm.

Damage under tension at high strain rate nucleates within the UFG volume and on the boundary between coarse grain and fine grain phases. Fracture of the RVE is a result of

stochastic damage nucleation and growth. Structure heterogeneity may influence on the random distribution of total plastic work over the RVE. Therefore, fracture of fine-grained alloys with a bimodal grain size distribution under dynamic tension has probabilistic character. The probability of microcracks nucleation within the RVE can be described by the Eq. [28]:

$$P_r(W^p)=1-exp\,[(\frac{W^p-W^p_{min}}{W^p_0})^{\alpha}\,],\ W^p \geq W^p_{min}\,, \tag{13}$$

where p_r is the Weibull probability function, W^p_{min} is the minimal possible total plastic work per unit volume at microscale level, α and W^p_0 are constant parameters of the distribution. The damaged RVE retains the resistance to plastic deformation during dynamic tension. Note that, for the light alloys with bimodal grain size distributions, the ultrafine-grained volume can be considered as a quasi-brittle phase, in which the microcracks are generated during the plastic deformation while the macroscopic mechanical behavior exhibit good ductility. Thus, density of microcracks of light alloys with a bimodal grain size distribution can be written by Eq. (14) which is similar to Eq. referenced in [29]:

$$N = N_0 P_r(W^p)=N_0\{1-exp\,[(\frac{W^p-W^p_{min}}{W^p_0})^{\alpha}\,]\},\ W^p \geq W^p_{min}\,, \tag{14}$$

where N is the density of microcracks, N_0 is the saturation density of microcracks at formation of mesoscopic crack.

Figure 4 shows the local damage distribution, mesocracks, total plastic work per unit volume under tension, and tension stress pattern at strain rate of 10^6 s^{-1} in RVE of UFG AMg6 aluminum alloy with a bimodal distribution of grain size for specific volume of coarse grains of ~75 % (See Fig. 1 (c)). The duration of tension corresponds to 0.2 μs. Mesocracks nucleated within the UFG volume may intersect coarse grains. Application of SPH method to multiscale simulation of fracture allows to estimate the bulk inelastic deformation caused by the crack opening.

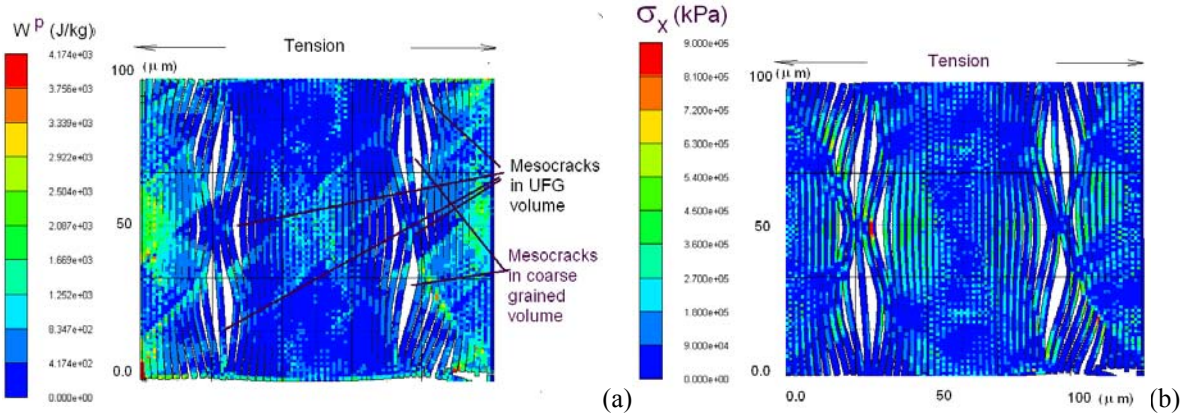

Fig. 4. Distribution of total plastic work per unit volume (a) and tensile stress (b) at in AMg6 aluminum alloy with coarse grain size of~20 μ and ultrafine grain size of~1 μm.

Fig. 5 shows distribution of total plastic work per unit volume within the RVE of AMg6 aluminum alloy under shock wave loading with amplitude of 3.2 GPa. The coarse grained specific volume of RVE is equal to ~50 %. Damages are localized in the UFG volume near the grain boundary of coarse grains under dynamic compression. Failure mechanisms of light

alloys with a bimodal grain size distribution have similarity at compression and tension loadings. Local damage nucleation of light alloys with a bimodal distribution of grains occurs in shear bands and zones of their intersection (See Fig. 3 and Fig.4). Therefore, fracture kinetics and sizes of fragments depend on the volume concentration of coarse grains.

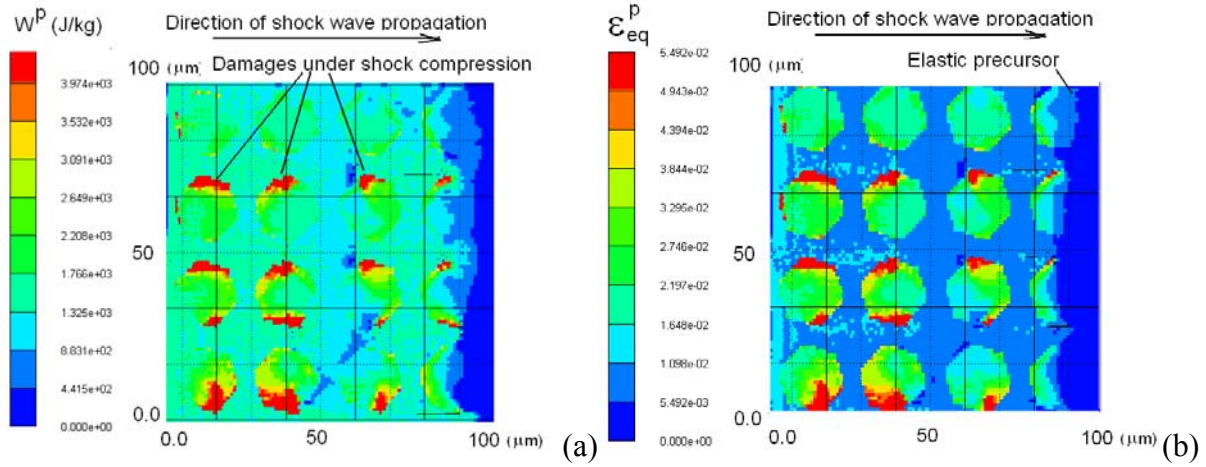

Fig. 5. Distribution of total plastic work per unit volume (a) in RVE under shock wave loading with amplitude of 3.2 GPa. Distribution of equivalent inelastic strain in AMg6 aluminum alloy with coarse grain size of~20 μ and ultrafine grain size of~1 μm (b).

It is significant that increases in fine precipitates concentration in light alloys cause the growth of resistance to plastic flow within both coarse and ultrafine grains. Fine precipitates in alloys not only affect the hardening but also lead to change the influence of the grain size distribution on volume concentration of shear bands.

The ductility of UFG light alloys increases when a relative part of coarse grains in volume is decreased. Fig. 6(a) shows the dependence of strain to fracture versus specific volume of coarse grains in Al-Mg alloy with a bimodal grain sizes distribution. Experimental data [8,11.12] denote by filled symbols. The curve displays the approximation of calculated data by the relation:

$$\varepsilon_f^n = 0.01 exp(C_{cg} / 0.363), \tag{15}$$

where ε_f^n is the strain to fracture under quasi-static tension, C_{cg} is the specific volume of coarse grain size.

Eq. (15) describes ductility of UFG Al-Mg alloys with a bimodal grains distribution versus the specific volume of coarse grains. UFG Al-Mg alloys have fine grain size of 1 μm and coarse grain size of 20 μm.

The increase in ductility of light alloys under quasi-static tension occurs when specific volume of coarse grains is greater than 30 %.

Fig. 6 (b) shows the dependence of strain to fracture of aluminum and magnesium alloys on logarithm of strain rates. Experimental data reported by Ulacia [30] for coarse grained magnesium alloy AZ31 are marked by filled simbols.

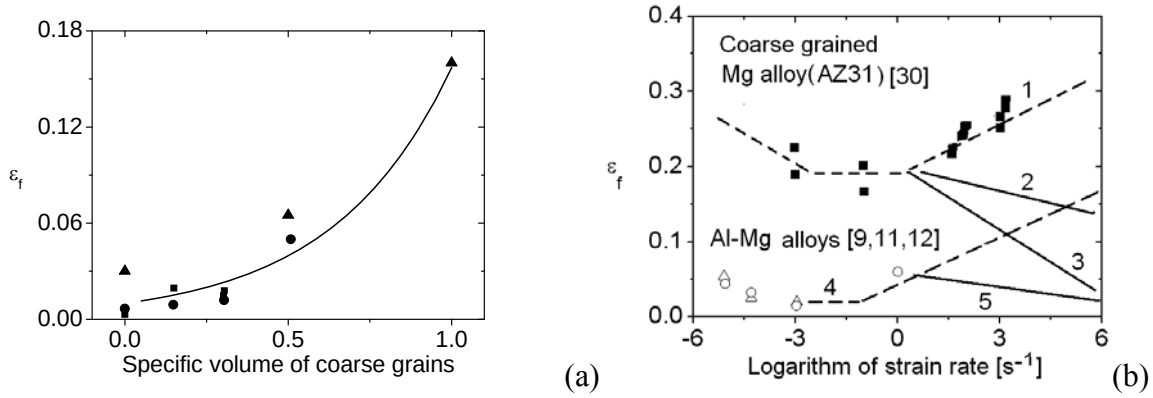

Fig. 6. The strain to fracture of Al-Mg alloy with a bimodal grain sizes distribution versus specific volume of coarse grains (a). Strain to fracture of aluminum and magnesium alloys vs logarithm of strain rates.

The curve 1 corresponds to approximation of experimental data on coarse grained AZ31 magnesium alloy. The curve 2 corresponds to approximation of calculated strain to fracture of Ma2-1 magnesium alloy with a bimodal grains structure for specific volume of coarse grains of 70 %. The curve 3 displays decreasing strain to dynamic fracture for magnesium alloy with a bimodal grains structure for specific volume of coarse grains of 10 %. The curve 4 shows increasing dynamic ductility of Al-Mg alloys with a bimodal grains structure. The curve 5 displays decreasing dynamic ductility of Al-Mg alloys with a bimodal grains structure for specific volume of coarse grains of 10 %.

4 CONCLUSIONS

The multiscale level approach of computer simulation was used for the simulation of fracture of magnesium and aluminium alloys at high strain rates. The model structured representative volumes (RVE) takes into account the influence of unimodal and bimodal grain size distributions and concentration of precipitates on mechanical properties of alloys.

Fracture of fine-grained alloys under dynamic loading has probabilistic character and depends on parameters of structure heterogeneity.

Formation of macro-scale failure zone is a result of several processes of structure evolution including damage nucleation, damage growth, and coalescence of damages.

Damage nucleation is associated with strain localization at mesoscale level. Results of computer simulation demonstrate that the high strain localization in UFG alloys under dynamic loadings depends on the ratio between volume concentrations of fine and coarse grains. Fine precipitates in alloys not only affect the hardening but also lead to change the influence of the grains size distribution on volume concentration of shear bands. The dynamic ductility of UFG light alloys is increased when specific volume of coarse grains is greater than 30 %. Results of computer simulation can be used for estimation of grains size distribution influence on the dynamic strength and ductility of UFG alloys processed by severe plastic deformation methods.

ACKNOWLEDGMENTS

This work is supported by Ministry of Sciences and Education of Russian Federation (State task №2014/223, project № 1943), also by the Grant from the President of the Russian Federation, and partially RFBR (project 08-08-12055). The authors are grateful for the support of this research.

REFERENCES

[1] Valiev, R.Z., Enikeev, N.A., Murashkin, M.Yu., et al. On the origin of the extremely high strength of ultrafine-grained Al alloys produced by severe plastic deformation. *Scripta Materialia.* (2010) **63:** 949–952.

[2] Pozdnyakov, V.A., Ductility of nanocrystalline materials with a bimodal grain structure. *Tech. Phys. Lett.* (2007). **33**: 1004–1006.

[3] Malygin, G.A., Strength and plasticity of nanocrystalline metals with a bimodal grain structure. *Phys. Solid State* (2008). **50**: 1032–1038.

[4] Prasad, M.J.N.V., Suwas, S., Chokshi, A.H., Microstructural evolution and mechanical characteristics in nanocrystalline nickel with a bimodal grain-size distribution. *Mater. Sci. Eng. A* (2009). **503**: 86–91.

[5] Ramtani, S., Dirras, G., Bui, H.Q., A bimodal bulk ultra-fine-grained nickel: experimental and micromechanical investigations. *Mech. Mater.* (2010). **42**: 522–536.

[6] Agnew, S.R., Horton, J.A., Lillo, T.M., Brown D.W. Enhanced ductility in strongly textured magnesium produced by equal channel angular processing. *Scripta Materialia* (2004) **50**: 77–381.

[7] Mukai T, Yamanoi M., Watanabe H. et al. Effect of grain refinement on tensile ductility in ZK60 magnesium alloy under dynamic loading. *Mater. Trans*. (2001) **42**: 1177-1181.

[8] Fan, G.J., Choo, H., Liaw, P.K., Lavernia, E.J., Plastic deformation and fracture of ultrafine-grained Al–Mg alloys with a bimodal grain size distribution. *Acta Mater*. (2006). **54**: 1759–1766.

[9] Ahn, B., Lavernia, E.J., Nutt, S.R., Dynamic observations of deformation in an ultrafine-grained Al–Mg alloy with bimodal grain structure. *J. Mater. Sci.* (2008) **43**: 403–7408.

[10] Lee, Z.H., Radmilovic, V., Ahn, B., Lavernia, E.J., Nutt, S.R., Tensile deformation and fracture mechanism of bulk bimodal ultrafine-grained Al–Mg alloy. *Metall. Mater. Trans. A*. (2010.) **41**: 795–801.

[11] Han, B.Q., Lee, Z., Witkin, D., Nutt, S.R., Lavernia, E.J., Deformation behavior of bimodal nanostructured 5083 Al alloys. *Metall. Mater. Trans. A*.(2005). **36**: 57– 965.

[12] Han, B.Q., Huang, J.Y., Zhu, Y.T., Lavernia, E.J.,. Strain rate dependence of properties of cryomilled bimodal 5083 Al alloys. *Acta Mater.* (2006) **54**: 3015–3024.

[13] Skripnyak, E. G., Skripnyak, and V.A., Skripnyak, V. V. Fracture of nanoceramics with porous structure at shock wave loadings. *Shock Compression of Condensed Matter. AIP Conf. Proc*. 2012. **1426**: 965 -970. doi: 10.1063/1.3686485.

[14] Skripnyak V.A. Mechanical behavior of nanostructured and ultrafine-grained materials under shock wave loadings. experimental data and results of computer simulation. *Shock Compression of Condensed Matter.* AIP Conf. Proc. (2012) **1426:** 965-970. doi: 10.1063/1.3686438

[15] Zhu, L., Lu, J. Modelling the plastic deformation of nanostructured metals with bimodal grain size distribution International. *J.l of Plasticity.* (2012) **30–31**: 166–184
[16] Joshi, S.P., Ramesh, K.T., Han, B.Q., Lavernia, E.J., Modeling the constitutive response of bimodal metals. *Metall. Mater. Trans. A*. 2006. **37**: 397–2404.
[17] Simchi, H., Simchi, A.,. Tensile and fatigue fracture of nanometric alumina reinforced copper with bimodal grain size distribution. *Mater. Sci. Eng. A* (2009). **507**: 200–206.
[18] Parshikov A.N., Medin S.A. Smoothed particle hydrodynamics using interparticle interparticle contact algorithms. *J. Comp. Phys.* (2002) **180**: 358-382.
[19] Parton, V.Z., Morozov, E.M. Mechanics of elastic-plastic fracture: Fundamentals of fracture mechanics. 2008. KomKniga . 400 p. ISBN: 978-5-484-01022-6.
[20] Casem D. T. and Dandekar D. P. Shock and mechanical response of 2139-T8 aluminum. *J. Appl. Phys*. (2012) **111**: 063508 doi: 10.1063/1.3694661.
[21] Clayton, J.D., McDowell, D.L. A multiscale multiplicative decomposition for elastoplasticity of polycrystals. *Int. J. of Plasticity* (2003) **19:**1401–1444.
[22] Frost, H.J., and Ashby, M.F. Deformation Mechanism Maps. The Plasticity and Creep of Metals and Ceramics, Pergamon Press, Oxford–New York–Toronto–Sydney–Paris–Frankfurt, 1982.
[23] Seidman, D.N., Marquis, E.A., Dunand D.C. Precipiation strengthening at ambient and elevated temperatures of heat-treateble Al (Sc) alloys. *Acta Meterialia*. (2002) **50**: 4021-4035.
[24] Herzig N., et.al., Modeling of mechanical behavior of ultra-fine grained titanium alloys at high strain rates, in Proc. 3-rd Int. Conf. on *High Speed Forming*. March 11-12, 2008. Dortmund, Germany. (2008): 141-150.
[25] Skripnyak V.A., et. al., Mechanical behavior of fine-grained metal alloys under dynamic loadings", in Proc. Int. Conf. *XI Khariton's Topical Scientific Readings*, 2007, Sarov, Russia. (2007):369-374.
[26] Herzig N., et.al., The mechanical behavior of ultra-fine grained Ti-8-22-22S over a wide range of strain rates, in Proc. 3-rd Int. Conf. on *High Speed Forming*, March, 11-12, 2008. Dortmund, Germany, (2008): 65-74.
[27] Skripnyak, V.A., Skripnyak, E.G., Deformation and fracture of UFG alloys under shock wave loadings. Computer simulation on the mesoscopic levels", in Proc. Int. Conference *Shock Wave in Condensed Matter*. Saint-Petersburg - Novgorod, 5-10, September. (2010): 319-322.
[28] Vinogradov, V., Hashin Z. Probabilistic energy based model for prediction of transverse cracking in cross-ply laminates. *Int. J. of Solids and Structures*. (2005) 42: 365–392.
[29] Zhu, L., Shi, S., Lu, K., Lu, J.A statistical model for predicting the mechanical properties of nanostructured metals with bimodal grain size distribution. *Acta Materialia*. (2012) **60**: 5762–5772.
[30] Ulacia I. et al. Tensile characterization and constitutive modeling of AZ31B magnesium alloy sheet over wide range of strain rates and temperatures. *J. of Materials Processing Technology*. (2011) **211**: 830–839.